

Clones and mutants in the evolution of angular momentum coherent states

P. Rozmej[†]

*Theoretical Physics Department, Institute of Physics,
University Maria Curie-Skłodowska, PL 20-031 Lublin, Poland
and
Institut des Sciences Nucléaires, F 38026 Grenoble-Cedex, France*

R. Arvieu*

*Institut des Sciences Nucléaires, F 38026 Grenoble-Cedex, France
(Received December 2, 2024)*

Angular momentum coherent states are generated from well adapted gaussian distributions. Some of these states coincide with wave packets proposed long time ago by Mostowski, others are simple and physically meaningful generalizations. The time evolution of these wave packets is studied for a diatomic molecule on the basis of the universal scenario discovered by Averbukh and Perelman. In the case which coincides with that of Mostowski, the wave packet is cloned around a mean circular trajectory. For other cases, the wave packet is deformed for each time previously called the time of partial revival. The fractional waves with forms different from the initial one are named mutants. Transitions of the shape of the wave packet occur periodically. One shape has a plane of symmetry, the other an axis of symmetry. The first symmetry is generated mainly by classical motion alone while the second one is due to the quantum spread. We have also constructed simple coherent states for a symmetric rotor which are applicable to molecules and nuclei. Their time evolution also shows a cloning mechanism for the rational ratio of moments of inertia. For irrational values of this ratio, the scenario of partial revivals completed by Bluhm, Kostelecky and Tudose is valid.

I. INTRODUCTION

This paper is devoted to the application of the results of Averbukh and Perelman [1,2] to the time evolution of a selection of angular momentum coherent states of simple rotating systems. In ref. [1] the authors indeed discovered a universal scenario of fractional revivals in the long term evolution of quantum wave packets of bounded system which goes beyond the correspondence principle. They established this scenario by expanding the bound states energies relevant to the wave packet up to the second order with respect to the mean energy, thus producing a local spectrum linear plus quadratic in one quantum number. For a well concentrated wave packet at the initial time they defined two time constants T_{cl} and $T_{rev} > T_{cl}$ such that the foregoing evolution of the wave packet is predicted as follows: for $0 < t < T_{cl}$, the wave packet spreads around the mean trajectory that can be associated with the underlying classical evolution while for $T_{cl} < t < T_{rev}$ the wave packet interferes with itself in such a way that for fractional times $t = (m/n)T_{rev}$ the wave packet is divided into q fractional wave packets. If n is even, $q = n/2$, if not, then $q = n$. The specificity of the system and that of the wave packet determines the shape of the fractional wave packets which are supposed to be spread regularly around the mean trajectory. At time $t = T_{rev}$, the wave packet is rebuilt either identical or only resemblant to the original one, depending on the importance of the neglected terms higher than quadratic. In some very specific cases, the fractional wave packets are clones of the initial one as studied in the most recent paper [3] and the revival is exact. This scenario has been validated in the most spectacular manner by several authors for a wave packet in a circular orbit of the hydrogen atom [4], see also [5] and by Boris et al. [6] for an elliptic orbit. It has been extended by Bluhm and Kostelecky [7] to a very long evolution with the demonstration of superrevivals due to the cubic terms. Examples of vibrational wave packets in anharmonic potential of simple molecule were also found since [8,9]. The scenario has been thereafter extended to cases where the energy depends on two quantum numbers [10]. Our work will also partly rely upon this last paper. A recent synthesis [11] contains most of the references on this topic while ref. [12] has been devoted to the definition of the experimental of wave packets in atomic physics and in molecular physics.

Our aim is to consider only angular wave packets for diatomic molecules and also for symmetric rotors and our purpose is to discuss the time evolution of few coherent states of the angular momentum. There is rather extensive literature on the coherent states. A full bibliography on this subject is found in ref. [13]. Large efforts have been made to build up such wave packets mainly in the context of group theory. Little effort, on the contrary, has been made to understand in detail their time evolution. Until the work of [1,2] it was not realized that they could evolve according to an universal scenario. For a diatomic molecule or for a symmetric rotor, the spectrum of which are quadratic in quantum number like for the systems discussed in [3,14], the universal scenario is exact and repeats with period T_{rev} . The main question is whether the fractional wave packets are clones or just resemblant to the initial ones. Despite all efforts to concentrate initially the wave packet in the best possible way, the quantum evolution destroys

this concentration (spatial localization) according to the rule formulated in [1]. We will show in this paper under which conditions the wave packets separate into clones and in which conditions there is a more restricted scenario of partial revivals. We will also show the existence of new fractional waves with different shapes that we call mutants. It is crucial to present a simple and physically meaningful picture of a coherent state and to decrease the number of its parameters to the minimum. One should keep in mind that a coherent wave packet has a classical content larger than the eigenstates of the angular momentum. Due to this property, it is possible to choose in the simplest manner the coherent wave packet as we will show below.

In section II we will define one parameter wave packet originally introduced by Mostowski [15] for a diatomic molecule. We will show how this wave packet can be generated from a gaussian wave packet in three dimensions. In section III we will compare Mostowski's wave packet to a coherent state obtained by Atkins and Dobson [16] using Schwinger [17] boson representation of spin $\frac{1}{2}$. We will show that they are indeed very similar. In section IV we will study the time evolution of Mostowski's wave packet and will see that it clones exactly.

In section V we will extend the wave packet studied in section II. We will use the method of generating angular momentum coherent state from a gaussian wave packet used in section II to consider other geometries as in ref. [19]. One of these geometries is particularly useful to understand the time evolution of wave packet of rotating nuclei, according to previous work of nuclear physicists on Coulomb excited nuclei [20,21]. The time evolution of these wave packets requires the consideration of two coupled variables (θ, ϕ) and presents time revivals but no cloning. A new and interesting regime of transition between two symmetries is found with the appearance of mutants. In the Appendix more general wave packets are considered which fulfill the minimum uncertainty relation. By varying one parameter (η) one obtains clones and mutants.

Finally in section VI, we will construct an angular momentum coherent state of a symmetric rigid rotor according to the rules defined by Janssen [18]. The time evolution of such a state is studied in section VII. Once the number of parameters is reduced, the time evolution of the coherent state, which is now a three dimensional system with two quantum numbers as in [10], presents clones if the ratio of the moments of inertia is rational. In the case when this ratio is not a rational number the fractional wave packets are not clones.

II. DERIVATION OF MOSTOWSKI'S COHERENT STATE FOR THE DIATOMIC MOLECULE

In this section, we will study the angular wave packet $\Psi_M(\theta, \phi)$ (normalized to unity) defined as follows

$$\Psi_M(\theta, \phi) = \sqrt{\frac{2N}{4\pi \sinh(2N)}} e^{N \sin \theta e^{i\phi}}. \quad (1)$$

Ψ_M depends on a single real parameter N . It coincides with the coherent state defined by Mostowski [15] who wrote it as:

$$\Psi_M(\theta, \phi) = C^{-\frac{1}{2}} e^{N(\vec{u}_1 + i\vec{u}_2) \cdot \vec{n}} \quad (2)$$

in terms of $\vec{n} = (\sin \theta \cos \phi, \sin \theta \sin \phi, \cos \theta)$, two other constant unit vectors \vec{u}_1, \vec{u}_2 perpendicular to each other and C a normalization constant. The form (1) is a particular case of (2) with \vec{u}_1 chosen along Ox and \vec{u}_2 along Oy .

We will now show that the wave packet (1) is also generated from a three dimensional gaussian wave packet $\Psi_G(r, \theta, \phi)$ written as

$$\Psi_G(r, \theta, \phi) = \frac{1}{(2\pi)^{\frac{3}{4}} \sigma^{\frac{3}{2}}} \exp \left[-\frac{(\vec{r} - \vec{r}_0)^2}{2\sigma^2} + i \frac{\vec{p}_0 \cdot \vec{r}}{\hbar} \right]. \quad (3)$$

Indeed (1) is obtained from (3) if one assumes:

$$\vec{r}_0 = \hat{x}x_0, \quad \vec{p}_0 = \hat{y}p_0, \quad \frac{x_0}{\sigma} = \frac{p_0\sigma}{\hbar} = \sqrt{N}. \quad (4)$$

The directions of \vec{r}_0 and \vec{p}_0 define respectively those of \vec{u}_1 and \vec{u}_2 . The mean angular momentum of (3) is then:

$$\langle \Psi_G | L_x | \Psi_G \rangle = \langle \Psi_G | L_y | \Psi_G \rangle = 0 \quad (5)$$

$$\langle \Psi_G | L_z | \Psi_G \rangle = x_0 p_0 = N\hbar. \quad (6)$$

Moreover, in order to get rid of the radial dependence in Ψ_G , one selects simply the constant radius $r = x_0 = \sqrt{N}\sigma$. The wave packet $\Psi_G(\sqrt{N}\sigma, \theta, \phi)$ differs from $\Psi_M(\theta, \phi)$ by a normalization constant which is easily calculated to be that written in eq. (1). Mostowski's coherent angular wave packet is then (up to a normalization factor) the intersection of a gaussian wave packet (such that $\vec{r}_0 = \sqrt{N}\sigma\hat{x}$, $\vec{p}_0 = \frac{\hbar\sqrt{N}}{\sigma}\hat{y}$) with the sphere of radius $r = \sqrt{N}\sigma$.

Let us now explain why $\Psi_M(\theta, \phi)$ is an angular momentum coherent state. If we place $\Psi_G(r, \theta, \phi)$ in a harmonic oscillator potential such that $\omega = \frac{\hbar}{m\sigma^2}$, one obtains $p_0 = m\omega x_0$. On the other hand

$$\langle \Psi_G | \frac{p^2}{2m} + \frac{1}{2}m\omega^2 x^2 | \Psi_G \rangle = N\hbar\omega. \quad (7)$$

The 3D wave packet $\Psi_G(r, \theta, \phi)$ represents the initial wave function of a particle which, if treated classically, would rotate on a circle of radius x_0 with velocity ωx_0 . The value of N corresponds, in the proper units, both to the angular momentum and energy of the particle. When time evolves the gaussian $\Psi_G(r, \theta, \phi; t)$ is known not to spread but to rotate, up to a phase factor. In this evolution, the intersection $\Psi_G(\sqrt{N}\sigma, \theta, \phi; t)$ of Ψ_G with the sphere of radius $\sqrt{N}\sigma$ conveniently normalized is simply: $\exp(-i\frac{3}{2}t)\Psi_M(\theta, \phi - \omega t)$ i.e. a rotated Ψ_M which do not spread either. The solid angle with which the width σ is observed from the centre of the sphere is for every time $\Omega = 4\pi/(4N + 1)$ and can be made as small as desired with a very large value of N .

A second and less trivial reason for considering $\Psi_M(\theta, \phi)$ as a coherent state relies on the uncertainty relations for the spread of the angular momentum components. One has indeed using standard algebra of angular momentum eigenstates and standard integrals

$$\Psi_M(\theta, \phi) = \sqrt{\frac{2N}{\sinh(2N)}} \sum_{I=0}^{\infty} \frac{(2N)^I}{\sqrt{(2I+1)!}} Y_I^I(\theta, \phi), \quad (8)$$

$$\langle \Psi_M | L_z | \Psi_M \rangle = N \coth(2N) - \frac{1}{2}, \quad (9)$$

$$\langle \Psi_M | L_z^2 | \Psi_M \rangle = N^2 - \frac{1}{2} \langle L_z \rangle, \quad (10)$$

$$\langle \Psi_M | L_x^2 | \Psi_M \rangle = \langle \Psi_M | L_y^2 | \Psi_M \rangle = \frac{\langle L_z \rangle}{2}. \quad (11)$$

(in units of \hbar and \hbar^2). These equations are generalized in the Appendix. Therefore

$$\Delta L_x^2 \Delta L_y^2 = \frac{1}{4} \langle L_z \rangle^2. \quad (12)$$

However, if N is large enough one has:

$$\langle \Psi_M | L_z | \Psi_M \rangle = N - \frac{1}{2} = \bar{I}. \quad (13)$$

It is remarkable that eq. (9) and eq. (13) differ from eq. (6) and that the difference is only $\hbar/2$ for large N . Property (12) expresses the condition of minimum uncertainty for the components of \vec{L} which is one of the properties of coherent states.

Let us also stress that (1) is obtained from (2) by a convenient choice of axis. In this condition, the expansion of Ψ_M into spherical harmonics involves only states with $m = l$. If \vec{u}_1 and \vec{u}_2 are chosen with a different orientation, the physical meaning of the resulting wave packet would be exactly the same as above, the dependence on θ and ϕ would be simply more complicated than eq. (1) since the spherical harmonic expansion would contain terms with various $m \neq l$. The choice of \vec{u}_1 and \vec{u}_2 implied in (1) simplifies the function of θ and ϕ and leads to the circular wave packet expansion (8).

The time evolution of $\Psi_M(\theta, \phi)$ for the diatomic molecule Hamiltonian will be studied in section IV. We will see there that despite the efforts to build a coherent state, its behaviour in time evolution is far from classical.

III. BOSON REPRESENTATION OF THE ANGULAR MOMENTUM COHERENT STATE

Based on Schwinger's work [17] several angular momentum coherent states have been constructed which rely upon boson representation of spin s . The case with $s = 1/2$ was first considered by Bonifacio et al. [22] and studied more extensively by Atkins and Dobson [16]. Mikhailov [23] has generalized this case to any spin integer or half integer. His work was complemented by Gulshani [24]. According to Mikhailov, a coherent state formed with $2s + 1$ bosons depends on 2 complex numbers called α_+ and α_- combined to define other complex constants α_{jm} by

$$\alpha_{jm} = \alpha_+^{j+m} \alpha_-^{j-m} \binom{2j}{j-m}^{\frac{1}{2}}, \quad (14)$$

for $j = 0, s, 2s, \dots, ps, \dots$ and $m = -j, -j+1, \dots, j-1, j$.

The coherent state, called generically $|\alpha s\rangle$, is expressed by

$$|\alpha s\rangle = \exp\left(-\frac{n^{2s}}{2}\right) \prod_{\mu} \exp(\alpha_{s\mu} a_{\mu}^{\dagger}) |0\rangle \quad (15)$$

$$= \exp\left(-\frac{n^{2s}}{2}\right) \sum_{j=0, s, \dots, ps, \dots}^{\infty} \sum_{m=-j}^j \frac{1}{\sqrt{p!}} \alpha_{jm} |jms\rangle, \quad (16)$$

$|0\rangle$ represents the vacuum, a_{μ}^{\dagger} ($\mu = -s, \dots, s$) is a creation operator of a boson of spin s , while the normalization constant depends on α_+ and α_- through

$$n^{2s} = (|\alpha_+|^2 + |\alpha_-|^2)^{2s} = \sum_{\mu} |\alpha_{s\mu}|^2. \quad (17)$$

The states $|jms\rangle$ are normalized states of angular momentum j constructed from the a_{μ}^{\dagger} [see Mikhailov for the full expressions]. The expansion (16) contains integer and half integer j for $s = 1/2$, it reduces to integer j for $s = 1$, for $s = 2$ only even j occurs etc.

Mikhailov has also calculated the expectation values of various operators which are expressed in terms of a_{μ}^{\dagger} and a_{μ} . Due to this technical simplification, the calculations of expectation values are easier than the work necessary to obtain formulas (9) to (12) in the case of the coherent state $\Psi_M(\theta, \phi)$. It is interesting to compare the properties of the state $|\alpha s\rangle$ to those of $\Psi_M(\theta, \phi)$. For this purpose, a simplification of the parametrization is needed. We take $\alpha_- = 0$ and $\alpha_+ = k = \text{real number}$, and the state $|\alpha s\rangle$ is now denoted simpler as $|ks\rangle$

$$|ks\rangle = \exp\left[-\frac{(k^2)^{2s}}{2}\right] \sum_{j=0, s, \dots, ps, \dots}^{\infty} \frac{1}{\sqrt{p!}} (k^2)^j |j = ps, m = j, s\rangle \quad (18)$$

$$= \exp\left(-\frac{k^{4s}}{2}\right) \exp[\alpha_{ss} a_s^{\dagger}] |0\rangle. \quad (19)$$

In the previous section, it was clear from the compact expression (2) given by Mostowski that the same physical state can be written by introducing three additional angles which are necessary to specify \vec{u}_1 and \vec{u}_2 . The proof that this freedom exists also in the boson representation was given by Mikhailov [23]. By a convenient choice of axis the state written in eq. (16) with $2s + 1$ bosons and two complex parameters can be brought to the simple form (18) with only one boson of spin s with $\mu = s$ and one parameter $\alpha_{ss} = \alpha_+^{2s} = k^{2s}$. Such a choice was also done by Atkins and Dobson [16] for the case $s = 1/2$. The matrix elements of the components of \vec{L} given below are a particular case of formulas given in ref. [16].

$$\langle ks | L_z | ks \rangle = s k^{4s}, \quad (20)$$

$$\langle ks | L_z^2 | ks \rangle = s^2 k^{4s} (k^{4s} + 1), \quad (21)$$

$$\langle ks | L_z^2 | ks \rangle = \langle ks | L_z^2 | ks \rangle = \frac{s}{2} k^{4s}, \quad (22)$$

$$\Delta L_x^2 \Delta L_y^2 = \frac{1}{4} \langle L_z \rangle^2. \quad (23)$$

These formulas and expansion (18) compared to formulas (8) to (12) show that $|ks\rangle$ do not coincide exactly with Mostowski's coherent state. For $s = 1/2$ Atkins and Dobson have proposed to truncate the sum over j in order to take into account only integer values of j . In this process the new state that we will call $|k, \frac{1}{2}\rangle_i$ (i for integer) needs to be normalized properly and the formulas (20) to (23) cease to be valid.

Our purpose is now to compare $\Psi_M(\theta, \phi)$ to $|k, \frac{1}{2}\rangle_i$. It is interesting to choose the parameters N and k in such a way that the approximation (13) is valid. Then using (20) one puts

$$\frac{1}{2}k^2 = N - \frac{1}{2}. \quad (24)$$

The comparison presented in Fig. 1 shows that the probability C_I^2 to find the partial wave Y_I^I in Ψ_M and in $|k, \frac{1}{2}\rangle_i$ is practically the same for $N = 20$. For smaller N and k (i.e. N of the order of unity) we have observed small but not meaningful differences. It is therefore possible if N is large enough to identify Mostowski's coherent state to the boson representation of spin 1/2 of Atkins and Dobson.

IV. CLONING OF Ψ_M FOR A DIATOMIC MOLECULE

A diatomic molecule is a good example to which we can apply the results of Averbukh and Perelman [1] since the spectrum is exactly quadratic. Let $\Psi_M(\theta, \phi, t)$ be the wave packet at time t deduced from (1) or (8). In such a case

$$\Psi_M(\theta, \phi, t) = \sqrt{\frac{2N}{4\pi \sinh(2N)}} \sum_{I=0}^{\infty} \frac{(2N)^I}{\sqrt{(2I+1)!}} Y_I^I(\theta, \phi) \exp(-iI(I+1)\omega_0 t), \quad (25)$$

where we are using

$$\omega_0 = \frac{\hbar}{2J_0}, \quad (26)$$

where J_0 is the moment of inertia of the molecule. According to ref. [1] two characteristic times are introduced

$$T_{cl} = \frac{2\pi}{\omega_0(2\bar{I}+1)}, \quad T_{rev} = \frac{2\pi}{\omega_0} = (2\bar{I}+1)T_{cl}. \quad (27)$$

The choice of the axis \vec{u}_1 and \vec{u}_2 introduces an important simplification in the time evolution of Ψ_M . Indeed the quantum motion can be entirely concentrated in the variable ϕ due to the separation of variables in Y_I^I . Using the notations of [1] and $\Phi = N\phi - N(N+1)\omega_0 t$ one has

$$e^{i(I\phi - I(I+1)\omega_0 t)} = e^{i\Phi} e^{ik(\phi - 2\pi \frac{t}{T_{cl}})} e^{-i2\pi \frac{t}{T_{rev}} k^2}, \quad (28)$$

where angular momentum I has been replaced by $k = I - \bar{I}$. The last exponent is now linearized near the time $t = \frac{m}{n}T_{rev}$

$$e^{-2i\pi k^2 \frac{m}{n}} = \sum_{s=0}^{l-1} a_s \exp(-2i\pi \frac{s}{l} k), \quad (29)$$

where $l = n/2$ if n is an integer multiple of 4 and $l = n$ in the other cases. For odd n or not multiple of 4 $|a_s| = \frac{1}{\sqrt{l}}$ and there are $q = l$ terms in the sum, while for n multiple of 4 only $q = \frac{n}{2}$ coefficients $|a_s|$ take this value and others are zero. See ref. [1] for the rule concerning the phase of a_s . Eq. (28) can be rewritten near $t = \frac{m}{n}T_{rev}$ as

$$e^{i(I\phi - I(I+1)\omega_0 t)} = e^{i\Phi} \sum_{s=0}^{l-1} a_s e^{ik(\phi - \frac{2\pi}{l}(t + \frac{s}{l}T_{cl}))} \quad (30)$$

and finally $\Psi_M(\theta, \phi, t)$ takes the form [1]

$$\Psi_M(\theta, \phi; t) = \sum_{s=0}^{l-1} a_s \Psi_{cl}(\theta, \phi, t + \frac{s}{l}T_{cl}). \quad (31)$$

This expansion shows that Ψ_M at time t is a superposition of q clones which are made by a proper rotation of Ψ_M at time 0 around the Oz axis. The fractional wave Ψ_{cl} is in this case

$$\Psi_{cl}(\theta, \phi, t) = e^{i\omega_0 t} \Psi_M(\theta, \phi - \omega_0 t, 0). \quad (32)$$

At this point a few remarks are possible:

- i) The cloning mechanism does not depend on the particular weights of each I -partial wave.
- ii) The angle θ does not play a role in the mechanism of cloning and revival.
- iii) The cloning mechanism would appear in a similar manner for arbitrary choices of \vec{u}_1 and \vec{u}_2 of eq. (2). θ and ϕ would then be coupled in such a way that the clones would be formed in the plane defined by \vec{u}_1 and \vec{u}_2 .

The time evolution of the wave packet corresponding to $N = 20$ is shown in Fig. 2 and Fig. 3. In Fig. 2 a convenient set of times have been chosen to show the probability density as a function of θ and ϕ just during the regime of spreading of the wave packet ($t < T_{cl}$) then for a few cloning times followed by the full revival for $t = T_{rev}/2$. In Fig. 3 a "carpet" is shown of the section $0 \leq t \leq T_{rev}/2$ of the probability density for $\theta = \pi/2$ which shows up to $q = 7$ clones.

The difference between Mostowski's coherent state with that created by Atkins and Dobson $|k, s = \frac{1}{2}\rangle_i$ is so tiny that it does not present any interest to be shown.

The interpretation of the cloning is possible in the framework of classical mechanics only within the ensemble interpretation in the same line as explained by authors of ref. [5].

V. OTHER COHERENT ANGULAR WAVE PACKETS DEDUCED FROM A GAUSSIAN

In this section we will extend somewhat the method of production of angular wave packets presented in section II which leads to Mostowski's coherent state in order to analyze the mechanism of cloning and to enrich the study of angular wave packets.

A. Wave packet deduced from a linear motion.

If we put $\vec{r}_0 = z_0 \hat{z}$, $\vec{p}_0 = 0$ in (3) we obtain a wave packet which moves in the harmonic oscillator along Oz . Its normalized intersection with the sphere $r = z_0 = \sigma\sqrt{N}$ is the simple wave packet

$$\Psi_0(\theta, \phi) = \sqrt{\frac{N}{2\pi \sinh(2N)}} e^{N \cos \theta} \quad (33)$$

$$= \sqrt{\frac{N}{2\pi \sinh(2N)}} \sum_{I=0}^{\infty} \sqrt{4\pi(2I+1)} \sqrt{\frac{\pi}{2N}} I_{I+1/2}(N) Y_0^I(\theta, \phi), \quad (34)$$

where $\sqrt{\frac{\pi}{2N}} I_{I+1/2}(N)$ is a modified spherical Bessel function of the first kind. This Ψ_0 is cylindrically symmetric around the Oz axis and could possibly represent the state of an excited diatomic molecule or of an axially symmetric rigid top with $K = 0$ (molecule or nucleus). Let us consider simply the first case and define the coefficient of $Y_0^I(\theta, \phi)$ in (34) as b_I

$$\Psi_0(\theta, \phi) = \sum_I b_I Y_0^I(\theta, \phi). \quad (35)$$

Although ϕ is put for completeness, this wave function depends only on θ . Let us now evolve $\Psi_0(\theta, \phi)$ with the hamiltonian of the diatomic molecule

$$\Psi_0(\theta, \phi; t) = \sum_I b_I e^{-i\omega_0 I(I+1)t} Y_0^I(\theta, \phi). \quad (36)$$

With the use of \bar{I} and k defined as

$$\bar{I}(\bar{I} + 1) = \sum_I |b_I|^2 I(I + 1) \quad k = I - \bar{I} \quad (37)$$

we have

$$T_{rev} = \frac{2\pi}{\omega_0} \quad T_{cl} = \frac{2\pi}{\omega_0} \frac{1}{2\bar{I} + 1}. \quad (38)$$

Using (29) it is not possible in this case to write $\Psi_0(\theta, \phi; t)$ as a superposition of clones, despite the fact that the energy spectrum is exactly quadratic. Indeed in (25) the ϕ dependence of Y_I^I was $e^{iI\phi}$ and therefore ϕ was associated with an angle of rotation around Oz , while in (34) the dependence in θ of Y_0^I is not exponential. Therefore, the present wave packet exhibits the limited scenario of partial revivals described by Averbukh and Perelman. The building block of the wave packet, noted as $\Psi_{cl}(\theta, \phi; t)$ is expressed as

$$\Psi_{cl}(\theta, \phi; t) = \sum_I b_I e^{-2i\pi I t/T_{cl}} Y_0^I(\theta, \phi). \quad (39)$$

The time evolution of $\Psi_0(\theta, \phi; t)$ is represented in Fig. 4. Since the wave packet is in fact one dimensional, the "carpet" representation provides the essential features of the time evolution. On a sphere areas of constant probability density could be represented by parallel circles centered on Oz axis. The quantity $2\pi \sin \theta |\Psi_{cl}|^2$ is represented in Fig. 5. This shows that the revival wave packets are rings on the sphere and, due to this special topology, do not clone the initial wave function. The pattern of the carpet shown in Fig. 4 is very much resemblant to that discussed recently for a special wave packet in one dimensional box in ref. [27]. Indeed there is a superposition of ridges and valleys with simple slopes as a function of t . The interpretation of this effect can be given in similar terms as in [27]. Note that the quantity plotted in Figs.4 and 5 has the same boundary conditions as the wave packet on the edge of the box. This produces a reflection effect in Fig. 4 totally absent in Fig. 3 since the boundary conditions are different on the circle.

B. Wave packet deduced from an elliptic motion.

A second extension of Mostowski's wave packet follows from the introduction of a new parameter η as follows. Let:

$$\vec{r} = x_0 \hat{x}, \quad \vec{p} = p_0 \hat{y} = \frac{\hbar \eta \sqrt{N}}{\sigma} \hat{y}. \quad (40)$$

Therefore

$$\langle \Psi_G | L_Z | \Psi_G \rangle = \eta N. \quad (41)$$

The corresponding classical motion is then elliptical in the xOy plane also for the harmonic oscillator. Our suggestion is to generate from it a more general coherent wave packet that will be applied to the diatomic molecule. Using Mostowski's notations, the corresponding wave packet obtained by normalized intersection of Ψ_G with the sphere $r = x_0 = \sigma \sqrt{N}$ is seen to be

$$\Psi_\eta(\theta, \phi) = C e^{N(\vec{u}_1 + i\eta \vec{u}_2) \cdot \vec{n}} \quad (42)$$

$$= \sqrt{\frac{2N}{4\pi \sinh(2N)}} \exp[N_1 \sin \theta e^{i\phi} + N_2 \sin \theta e^{-i\phi}]. \quad (43)$$

New variables N_1 and N_2 are defined from N and η as

$$N_1 = N \frac{1 + \eta}{2}, \quad N_2 = N \frac{1 - \eta}{2}. \quad (44)$$

Expanding the gaussians in spherical harmonics leads to the new partial wave expansion:

$$\Psi_\eta(\theta, \phi) = \sum_{LM} b_{LM}(N_1, N_2) Y_M^L(\theta, \phi), \quad (45)$$

$$b_{LM}(N_1, N_2) = \sqrt{\frac{2N}{\sinh(2N)}} \sum_{l'} \frac{(-1)^l (2N_1)^l (2N_2)^{l'}}{\sqrt{(2l)!(2l')!}} \frac{\langle ll'00|L0\rangle \langle ll'l-l'|LM\rangle}{\sqrt{2L+1}}. \quad (46)$$

The coefficient b_{LM} is here expanded in terms of Clebsch–Gordan coefficients. The average of L_z is now simply

$$\langle \Psi_\eta | L_z | \Psi_\eta \rangle = \eta \left[N \coth(2N) - \frac{1}{2} \right]. \quad (47)$$

For $\eta = 0$, the wave packet coincides with the one defined by (34) with the direction Oz replaced by Ox . For $\eta = 1$, it coincides with (1). Using the results derived in the Appendix one obtains the following average values

$$\langle L_x^2 \rangle = \frac{1}{2} \eta^2 [N \coth(2N) - \frac{1}{2}] \quad (48)$$

$$\langle L_y^2 \rangle = \frac{1}{2} [N \coth(2N) - \frac{1}{2}]. \quad (49)$$

From (48,49) one sees that eq. (12) is extended to cases such that $\eta \neq 1$. On the other hand, the total uncertainty provides a spread of the partial waves that is strongly dependent on η since:

$$\begin{aligned} \Delta L_\eta^2 &= \langle L^2 \rangle - \langle L_z \rangle^2 \\ &= (N \coth(2N) - \frac{1}{2}) + \eta^2 [N^2 - N \coth(2N)(N \coth(2N) - \frac{1}{2})], \end{aligned} \quad (50)$$

with the simpler limit for large N

$$\Delta L_\eta^2 = N - \frac{1}{2} + \eta^2 \frac{N}{2}. \quad (51)$$

With the consideration of the ensemble of states (42), (46) we are considering for fixed N a collection of states which, for $t = 0$, have exactly the same probability density as a function of θ and ϕ because one has indeed

$$|\Psi_\eta(\theta, \phi)|^2 = \frac{2N}{4\pi \sinh(2N)} \exp(N \sin \theta \cos \phi). \quad (52)$$

This result is obvious from the geometric construction which allows to generate (42) from (3): the probability density of the gaussian (3) in space is independent of p_0 . Its intersection with the sphere has also this property. From this procedure, one is able to generate, for given N , a one parameter family of states associated to the diatomic molecule. Among these states only the state $\eta = 1$ has a classical analog corresponding to the classical rotation.

C. Time evolution of the coherent state deduced from elliptic motion.

It is interesting to compare the time evolution of the states in one family. Clearly the two values $\eta = 1$ and $\eta = 0$ studied previously, constitute limiting cases with a very different geometry. For $\eta = 1$, the time evolution is reported on the ϕ motion with Oz as an axis of symmetry. For $\eta = 0$, the wave is axially symmetric along Ox and the time evolution concerns only the angle (analogous to θ) with respect to Ox . For other values of η , the wave packet contains many values of I and for each I only spherical harmonics for which M has the same parity as I have non zero components in the expansion (46) and the spread of I is minimum for $\eta = 0$. It is therefore expected that the comparison of the time evolution will reflect this increase of complexity.

The autocorrelation functions for few values of η studied in Fig. 6 for $N = 20$ confirm the previous analysis. For the smaller value of η , the behaviour is somewhat poor since ΔL_η^2 increases from 19.5 for $\eta = 0$ to 29.5 for $\eta = 1$. We can measure the angular aperture corresponding to the intersection of the probability density of $|\Psi_G|^2$ with the sphere of radius $r = \sigma\sqrt{N}$ by the solid angle $\Omega = 4\pi/(4N+1)$ corresponding to the cone defined by $\tan \frac{\alpha}{2} = \frac{1}{2\sqrt{N}}$. The time of spreading τ_η of this wave packet of width ΔL_η (51) is of the order of

$$\tau_\eta = \frac{2\pi}{\omega_0} \frac{1}{\Delta L_\eta}. \quad (53)$$

The difference in spreading with η is clearly seen in the autocorrelation functions represented in Fig. 6. We can also define maximum number of fractional wave packets that can be observed knowing that $\tan \frac{\alpha}{2} = \frac{1}{2\sqrt{N}}$ as

$$q_{max} = \frac{\pi}{\arctan(1/2\sqrt{N})}. \quad (54)$$

This number is confirmed by the observation of the 'carpet' of Fig. 3 for $N = 20$ for which we have up to 7 clones. The lifetime τ'_η of a system of q fractional wave packets can be estimated as

$$\omega_0 \tau'_\eta \Delta L_\eta = \frac{2\pi}{q}. \quad (55)$$

Also in Fig. 3 one sees clearly for $q = 2, 3$ the large intervals of time during which clones are observed.

For the general elliptic wave packet, as deduced from the previous discussion there are no clones, but partial revivals with different topology. Due to the change of symmetry, it is indeed necessary to make a smooth transition between a system of clones located for $\eta = 1$ in the Oxy plane and a system of rings which were discussed at the end of subsection V A. In the system of coordinates adopted in subsection V B and corresponding to $\eta = 0$ these rings have Ox as symmetry axis. The transition from the clones for $\eta = 1$ to the rings for $\eta = 0$ is made by developing for η smaller than 1 a system of pairs of crescents perpendicular to the Oxy plane. This transition is clearly visible for particular fractional revival times in Fig. 7. For a very small value of η the upper part and the lower part of one crescent meet the corresponding parts of a symmetric crescent in order to build up such a ring symmetric around Ox . Again this change of topology of this construction forbids the cloning of all fractional waves. Most of them revive in shapes different from that of the initial wave packet. We propose to call these fractional wave packets mutants. Example of time evolution of wave packet with $\eta = 0.5$ is given in Fig. 8. It is well seen both in Fig. 8 and in Fig. 7 that clones and mutants can occur in the same time. For example for $\eta = \frac{1}{4}$ and $t = \frac{1}{3} T_{rev}$ there is a fractional revival at $\theta = \frac{\pi}{2}$ and $\phi = 0$ with the same shape as the initial wave packet and two crescents which almost close. This situation is similar to that which exists for $\eta = 0$ also for $t = \frac{1}{3} T_{rev}$. For $\eta = \frac{1}{2}$ and $t = \frac{1}{6} T_{rev}$ the two crescents do not form a ring. Among the three fractional waves which are present there are two which are identical to each other but with larger spread in θ . For this value $\eta = \frac{1}{2}$, there are three different topologies for the five fractional waves. In other publications on a different system [19], we had already found the transition from a gaussian three dimensional wave packet to a vortex ring. Refs. [19] were devoted, as well as our previous works, for the time evolution of such coherent waves in the case where the hamiltonian contains a spin orbit interaction in addition to the harmonic oscillator potential. If the spin is oriented along the initial wave packet displacement (Ox axis), the cylindrical symmetry is imposed on the system and preserved during evolution, a vortex rings appear.

The transition between the two shapes of fractional wave packets can be explained by comparing, as a function of η , the spread of the angle θ to the spread of the angle ϕ . If $\eta = 0$ the wave packet has no privileged direction on the sphere. It spreads therefore equally. In the case when $\eta = 1$ the wave packet is peaked near the plane with $\theta = \frac{\pi}{2}$ and the spread in θ is strongly reduced. The spread in ϕ is seen in the scenario of cloning in the plane xOy . For intermediate values of η , there is a competition between the two effects which manifests itself most strongly in the shape of the fractional waves.

For $\eta > 1$ (results not presented) we have observed a strong reduction of the spread in θ . For particular values of $\frac{m}{n}$, some mutants can be peaked with higher amplitude than their neighbours. This is in direct connection to the increase in p_0 which was necessary in the initial wave packet.

In the Appendix we have proved that most of the results obtained for the wave packet (42) hold also (at least qualitatively) for any function of the same argument as the exponential.

VI. COHERENT STATES FOR A SYMMETRIC TOP

It is natural to enlarge our previous study to rotational coherent states of symmetric tops which contain an additional degree of freedom. There are several possibilities in the literature for constructing such a state. Our aim is again to choose the axis of coordinates in order to eliminate irrelevant parameters and to make evolution understandable. This is possible only in the case of symmetric top. We will assume that the moments of inertia in the intrinsic frame $J_x = J_y$ and introduce the parameter δ such that:

$$\delta = \frac{J_x}{J_z} - 1. \quad (56)$$

The energy spectrum is then:

$$E(I, K) = \frac{\hbar^2}{2J_x} [I(I+1) + \delta K^2]. \quad (57)$$

A convenient rotational wave packet was defined and studied by Janssen [18] on the basis of the work of Perelomov [25] and Schwinger [17]. This wave packet denoted by three complex numbers x, y and z is a mixture of D_{MK}^I functions

$$|xyz\rangle = \exp\left(-\frac{1}{2}yy^*(1+xx^*)(1+zz^*)\right) \times \sum_{IMK} \sqrt{\frac{(2I)!}{(I+M)!(I-M)!(I+K)!(I-K)!}} x^{I+M} y^{2I} z^{I+K} |IMK\rangle. \quad (58)$$

The sum over I contains integer as well as half integer values of I i.e. this state extends that presented by Atkins and Dobson. On a similar line as in section III we call $|xyz\rangle_i$ its normalized projection onto the space with integer I . A particularly convenient choice of x, y and z as well as of the system of coordinates decreases the number of parameters to two and reduces the summation to I and K only. The simpler wave packet is then:

$$|r, \lambda\rangle = \exp(-r) \sum_{IK} (2r)^I \frac{(\sin \frac{\lambda}{2})^{I+K} (\cos \frac{\lambda}{2})^{I-K}}{\sqrt{(I+K)!(I-K)!}} |I- IK\rangle. \quad (59)$$

If L_X, L_Y, L_Z are the components of \vec{L} in the intrinsic axes, L_x, L_y, L_z those related to the laboratory axes, one has according to Janssen:

$$\langle r\lambda|L_x|r\lambda\rangle = \langle r\lambda|L_y|r\lambda\rangle = 0, \quad \langle r\lambda|L_z|r\lambda\rangle = -r, \quad (60)$$

$$\langle r\lambda|L_Z|r\lambda\rangle = -r \cos \lambda, \quad \langle r\lambda|L_X|r\lambda\rangle = r \sin \lambda, \quad \langle r\lambda|L_Y|r\lambda\rangle = 0, \quad (61)$$

$$\langle r\lambda|L^2|r\lambda\rangle = r\left(r + \frac{3}{2}\right). \quad (62)$$

The expansion (59) of the rotational coherent states in terms of $|I- IK\rangle$ has the same coefficients as the expansion of Atkins–Dobson in terms of angular momentum eigenstates $|IK\rangle$. The two expansions are connected by defining α_+ and α_- as:

$$\alpha_+ = \sqrt{2r} \sin \frac{\lambda}{2}, \quad \alpha_- = \sqrt{2r} \cos \frac{\lambda}{2}. \quad (63)$$

The projection $|r, \lambda\rangle_i$ deduced by restricting (59) to integer values of I and K verify eqs. (60) to (62) only approximately. However if r is large enough, these equations are obtained in a very good approximation. The time evolution of the wave packet $|r, \lambda\rangle_i$ will be studied in the next section for a rigid body symmetric rotor.

VII. TIME EVOLUTION OF JANSSEN'S COHERENT STATE

The energy spectrum of the axially symmetric rigid rotor is written as:

$$E_{IK} = \hbar\omega_0 [I(I+1) + \delta K^2]. \quad (64)$$

We will study the time evolution of a wave packet deduced from (59) with $\omega_0 = \hbar/(2J_x)$ and with average values

$$\langle r\lambda|L_Z|r\lambda\rangle = \bar{K} \simeq -r \cos \lambda \quad (65)$$

$$\langle r\lambda|L_z|r\lambda\rangle = \bar{I} \simeq -r. \quad (66)$$

The energy E_{IK} is written by taking \bar{K} and \bar{I} as reference, and defining k_1 and k_2 as:

$$k_1 = I - \bar{I} \quad k_2 = K - \bar{K}. \quad (67)$$

$$E_{k_1 k_2} = \hbar\omega_0 [\bar{I}(\bar{I}+1) + \delta \bar{K}^2] + \hbar\omega_0 (2\bar{I}+1)k_1 + \hbar\omega_0 \delta (2\bar{K})k_2 + \hbar\omega_0 k_1^2 + \hbar\omega_0 \delta k_2^2. \quad (68)$$

We now follow the lines drawn by Bluhm, Kostelecky and Tudose [10] who have considered the time evolution of a system which depends quadratically on two quantum numbers, in our case I and K . There are 4 time constants; the first pair defined as

$$T_{cl}^I = \frac{2\pi}{\omega_0(2\bar{I}+1)} \quad T_{rev}^I = \frac{2\pi}{\omega_0} = (2\bar{I}+1) T_{cl}^I \quad (69)$$

is related to the motion around Oz axis (laboratory axis), i.e. it is connected to the Euler angle α , the second pair plays a parallel role, it concerns the motion around the symmetric OZ axis and the Euler angle γ

$$T_{cl}^K = \frac{2\pi}{\omega_0\delta 2\bar{K}} = \frac{1}{\delta} \frac{2\bar{I}+1}{2\bar{K}} T_{cl}^I \quad T_{rev}^K = \frac{2\pi}{\delta\omega_0} = \frac{1}{\delta} T_{rev}^I. \quad (70)$$

The system of coordinates and the parametrization in (59) enables to profit by the separation of variables in the state $|I - IK\rangle$ since:

$$\langle\alpha\beta\gamma|I - IK\rangle = e^{i\alpha I} d_{-IK}^I(\beta) e^{-i\gamma K} = D_{-IK}^I(\alpha, \beta, \gamma). \quad (71)$$

The wave packet (59) at time t with conditions (65) and (66) and integer I and K will be denoted as $|\bar{I} \bar{K}\rangle$ and written as:

$$\langle\alpha\beta\gamma|\bar{I} \bar{K}\rangle_t = \sum_{IK} C_{IK}(r, \lambda) d_{-IK}^I(\beta) e^{i[\alpha I - 2\pi I(I+1)t/T_{rev}^I]} e^{-i(\gamma K + 2\pi K^2 t/T_{rev}^K)} \quad (72)$$

$$= e^{-i[\bar{I}(\bar{I}+1) + \delta\bar{K}^2]t/T_{rev}^I} \sum_{k_1 k_2} C_{k_1 k_2}(r, \lambda) d_{k_1 k_2}^I(\beta) \quad (73)$$

$$\times e^{i[\alpha k_1 - 2\pi(k_1/T_{cl}^I + k_1^2/T_{rev}^I)t]} e^{-i[\gamma k_2 + 2\pi(k_2/T_{cl}^K + k_2^2/T_{rev}^K)t]}.$$

The summation on I and K has been changed to a sum over k_1 and k_2 and the coefficient $C_{IK} d_{-IK}^I$ has been given the new indexes. The discussion of the time evolution of (73) follows in a straightforward manner that given by Bluhm, Kostelecky and Tudose [10]. The crucial parameter is δ . If T_{rev}^K and T_{rev}^I are not commensurate there is no cloning, however for $t = (m/n)T_{rev}^I$ there are partial revivals in the variable α : i.e. the wave packet is a superposition of q fractional wave packets peaked regularly along the Oz axis. ($q = (n/2)$ if n is even, n in other cases). For $t = (m'/n')T_{rev}^K$ the same scenario of partial revival occurs but this time there are q' fractional wave packets peaked around the OZ axis. [$q' = (n'/2)$ if n' is even, n' otherwise].

The interesting situation of commensurability of T_{rev}^I and T_{rev}^K allows, on the contrary, the construction of q^2 clones for all the time such that

$$t = \frac{m}{n} T_{rev}^{I,K} \quad (74)$$

The revival time $T_{rev}^{I,K}$ is the least common multiple of T_{rev}^I and T_{rev}^K

$$p T_{rev}^I = r T_{rev}^K = T_{rev}^{I,K}. \quad (75)$$

The time evolution of the rotational wave packets is presented in Fig. 9 and Fig. 10.

The particular choice $\bar{K} = 0$ leads to $T_{cl}^K = \infty$ but T_{rev}^K is finite as well as T_{cl}^I and T_{rev}^I . For the smaller value of t , the behaviour of the wave packet around Oz and OZ is different as seen from Fig. 10. There is indeed a classical rotation and spreading around Oz while no rotation occurs around OZ , only the spreading is observed around this axis.

Fig. 9 illustrates the case of an irrational value of δ where there are partial revivals for times $t = (m/n)T_{rev}^I$ around Oz and for times $t = (m'/n')T_{rev}^K$ where the revivals are around OZ . Note that the concentration of the wave packet for some definite values of α (or γ) has no influence on the other variable γ (or α) respectively.

Fig. 10 illustrates the case of a rational value of δ , for which there are q^2 clones. The proof that there are q^2 clones if condition (75) holds is rather simple, one applies twice the method of Averbukh and Perelman to linearize the exponential containing k_1^2 and k_2^2 in eq. (73).

Finally we want to stress that the variable β does not play a role in the time evolution. Obviously this is due to our particular choice of axis in eq. (59). The role played by β for the axial rotor is similar to the role played by θ in the diatomic molecule. With the other parametrization, as said at the end of section II the cloning would appear and we would need to couple θ and ϕ in order to explain in which particular direction the clones take place.

VIII. CONCLUSIONS

We have discussed the time evolution of angular momentum coherent states that were constructed by a simple, purely geometric, generating procedure. The basic ingredients are the three dimensional gaussian wave packets of the harmonic oscillator. We have used two of the parameters of the gaussian to derive an ensemble of coherent states which depend finally on two parameters N and η . The angular distribution of the probability density depends only on N , while the momentum distribution depends both on N and η . The uncertainty relations (12) are valid for all N and η . Such a variety of wave packets do not arise from the previous works on angular momentum coherent states with bosons. It is for example simple to show [21] that there is no place in the Atkins and Dobson or Mihailov's work for the wave packets (34) which correspond to $\eta = 0$. Also the coefficient α_{jm} defined by (14) in terms of α_+ and α_- cannot be put generally in the form such that (46) which ensures that b_{IM} is zero if I and M have an opposite parity.

In the framework of the scenario of ref. [1] we have shown that for $\eta = 1$ the wave packets spread at $t = \frac{m}{\hbar} T_{rev}$ into clones. However, the difference between the symmetries for $\eta = 0$ and $\eta = 1$ necessitates a change in the topology of the fractional wave packets. This change is such that these wave packets can be named mutants after a certain amount of deformation of their shape. It is a challenging question to find a proper way to excite such wave packets in a rotational band of a molecule or of a deformed nuclei.

The wave packets with $\eta = 0$ or wave packets with $M = 0$ have been already considered several times. In a reference work on Coulomb excitation of nuclei with heavy ions R.A. Broglia and A. Winther [20] have shown that such wave packets are generated in backward scattering. Their population of the excited states of a rotational band with $K = 0$ do not coincide with the very simplified expression (34). Indeed interference effects during the excitation process modulates this population to a large extent (Fig. 8, p.82 of ref. [20]). However, we have studied the time evolution of such a wave packet and this will be the subject of a future publication [29].

The authors of ref. [21] have written an important analysis on coherent rotational states, completing the work of [20]. They have already used the wave $|k, \frac{1}{2}\rangle_i$ of section III derived from [16], and they have also considered an extension toward other symmetries like $Sp(2, R)$, $Sp(4, R)$. Time evolution was studied but only for the average values of operators like quadrupole moments. The physical systems considered were the nucleus ^{238}U and the molecule CS_2 . The time evolution of expectation values of more general operators for wave packets due to quadratic dependence was studied in [26]. The operators studied in ref. [21] have very strict selection rules and the time evolution reflected these in much poorer behaviour than what is exhibited by the full wave packet and by the average values of the more complex observables [26] related to the position. It is, however, clear that all the wave packets considered in ref. [21] must evolve according to the scenario of ref. [1] with a very rich sequence of changes of shapes.

Finally, let us mention that the population of a set of rotational states of a molecule excited by an intense lasers has also been calculated recently [28]. However, the number of states excited in this way is small and it does not seem that in such a way the wave packet will concentrate so sharply on the sphere as we showed for $\eta = 0$ and $N = 20$.

Aronstein and Stroud [3] have shown "that, the infinite square well is an ideal system for fractional revivals since all wave functions exhibit fractional revivals of all orders". The same statement applies to the case of the diatomic molecule but is limited however to circular wave packets, i.e. to those which contain only $M = I$ partial waves in a convenient system of axis. The generation mechanism used in this paper can be extended to shapes different from gaussian distribution. Clones will always result in this particular condition. For the wave packets which contain populations of sublevels $M \neq I$, mutants will appear. All these results hold independently on the realization of the uncertainty condition (12). For systems where energy is quadratic in one quantum number we have shown that the time evolution can exhibit a rich structure of cloning and mutation of fractional revivals.

Our final study on the axially symmetric top is another illustration of the work of ref. [10]. We have made no effort here to generate mutants in this case although there is a possibility to enrich wave packets derived from Janssen's work [18].

In perspective of future work it would be interesting to look experimentally for the existence of mutants discussed in this paper. This requires observation both in space and in time. On the other hand, the scenario of Averbukh and Perelman should be extended to other symmetry breaking.

Acknowledgements

We want to thank C. Gignoux for his warm interest and remarks during this work. One of us (P.R.) acknowledges financial support from Centre National de la Recherche Scientifique.

APPENDIX A:

In this appendix we will extend the properties derived formerly in sections II and V to more general wave packets. Instead of the exponential function (42) we will study angular wave packets which are square integrable and derivable

functions of the argument v defined as

$$v = N(\vec{u}_1 + i\eta\vec{u}_2) \cdot \vec{n} . \quad (\text{A1})$$

There is no lack of generality in choosing \vec{u}_1 along Ox and \vec{u}_2 along Oy , therefore

$$v = N \sin \theta (\cos \phi + i\eta \sin \phi) . \quad (\text{A2})$$

We can write also Ψ in terms of x, y, z and r as

$$\Psi = \Psi(v) = \Psi\left(N\frac{x}{r} + i\eta N\frac{y}{r}\right) . \quad (\text{A3})$$

The derivative with respect to v is denoted simply

$$\Psi' = \frac{d\Psi}{dv} . \quad (\text{A4})$$

By partial derivations of (A3) we obtain

$$(L_x + i\eta L_y)\Psi = 0 . \quad (\text{A5})$$

This equation generalizes the property of the circular wave packet ($\eta = 1$)

$$L_+\Psi = 0 \quad (\text{A6})$$

to any value of the parameter η . The result of the application of L_x on Ψ is

$$L_x\Psi = -\cos\theta\eta N\Psi' , \quad (\text{A7})$$

while operating with L_z gives

$$L_z\Psi = N \sin \theta (\eta \cos \phi + i \sin \phi) \Psi' . \quad (\text{A8})$$

Therefore

$$\langle \Psi | L_z | \Psi \rangle = N \langle \Psi | \sin \theta (\eta \cos \phi + i \sin \phi) | \Psi' \rangle , \quad (\text{A9})$$

$$\langle \Psi | L_x | \Psi \rangle = -\eta N \langle \Psi | \cos \theta | \Psi' \rangle . \quad (\text{A10})$$

Since Ψ and Ψ' are both functions of $\sin \theta$ the integration over θ of the matrix element of $\cos \theta$ is zero. Therefore

$$\langle L_x \rangle = \langle L_y \rangle = 0 \quad (\text{A11})$$

and

$$\Delta L_x^2 = \langle L_x^2 \rangle = \eta^2 N^2 \langle \Psi' | \cos^2 \theta | \Psi' \rangle . \quad (\text{A12})$$

Using (A5) one finds also that

$$\Delta L_y^2 = \langle L_y^2 \rangle = N^2 \langle \Psi' | \cos^2 \theta | \Psi' \rangle . \quad (\text{A13})$$

A connection between matrix elements in (A13) and (A9) is found noting that

$$\frac{1}{\eta} L_x^2 \Psi = -i L_x L_y \Psi , \quad (\text{A14})$$

$$\eta L_y^2 \Psi = i L_y L_x \Psi . \quad (\text{A15})$$

Therefore

$$\left(\frac{1}{\eta} L_x^2 + \eta L_y^2\right) \Psi = L_z \Psi , \quad (\text{A16})$$

and finally

$$\frac{1}{\eta} \langle \Psi | L_x^2 | \Psi \rangle + \eta \langle \Psi | L_y^2 | \Psi \rangle = \langle L_z \rangle . \quad (\text{A17})$$

Inserting the results (A12), (A13) and (A9) into (A17) one obtains

$$2\eta N^2 \langle \Psi' | \cos^2 \theta | \Psi' \rangle = N \langle \Psi | \sin \theta (\eta \cos \phi + i \sin \phi) | \Psi' \rangle . \quad (\text{A18})$$

From this not obvious result one finds for every Ψ of the form (A3)

$$\Delta L_x^2 \Delta L_y^2 = \frac{1}{4} \langle L_z \rangle^2 . \quad (\text{A19})$$

The equation (A17) enables to understand the occurrence of $[N \coth(2N) - \frac{1}{2}]$ in equations (47), (48), (49) of the main text. For the case where $\Psi(v)$ takes the form of the exponential (42) the square of the wave function $|\Psi_\eta|^2$ and its derivative $|\Psi'_\eta|^2$ are independent of η . For a more general $\Psi(v)$ these simplifications do not hold but eqs. (A18) and (A19) are still valid.

Let us finally state that the geometric construction by which eq. (42) was derived from a three dimensional gaussian wave packet (3) cannot be generalized to non gaussian distributions. Indeed starting from

$$\Psi(r, \theta, \phi) = f(\vec{r} - \vec{r}_0) e^{\frac{i}{\hbar} \vec{p}_0 \cdot \vec{r}} , \quad (\text{A20})$$

where $f(\vec{r} - \vec{r}_0)$ is an arbitrary function, one does not obtain a function of the type (A3) by taking its normalized intersection with a sphere, except for $p_0 = 0$ and $\eta = 0$. However equation (A3) contains very large freedom outside the range of gaussian distributions. It is possible to choose Ψ in order to represent a well peaked distribution on the sphere while keeping eq. (A19).

To study the time evolution of $\Psi(v)$ a partial wave expansion is needed. It is obvious that all circular wave packets with $\eta = 1$ verify (A6) and contain only spherical harmonics Y_l^I . These wave packets exhibit perfect cloning as in ref. [3] because, as for (32), one has

$$\Psi_{cl}(N \sin \theta [\cos \phi + i \eta \sin \phi]; t) = e^{i\omega_0 t} \Psi(N \sin \theta [\cos(\phi - \omega_0 t) + i \eta \sin(\phi - \omega_0 t)]) , \quad (\text{A21})$$

On the other hand for $\eta = 0$ the symmetry is as described as for the exponential $\Psi(v)$: rings are formed around the Ox axis at times $t = \frac{m}{n} T_{rev}$. A transition between $\eta = 0$ and $\eta = 1$ occurs in a way similar to that described in the main text. However the detailed shapes of mutants depend on the precise form adopted for $\Psi(v)$.

-
- * E-mail: arvieu@isn.in2p3.fr
- † E-mail: rozmej@tytan.umcs.lublin.pl and rozmej@isnhp1.in2p3.fr
- [1] I.S. Averbukh and N.F. Perelman, Phys. Lett. A **139** 449 (1989).
- [2] I.S. Averbukh and N.F. Perelman, Usp. Fiz. Nauk. **161** 41 (1991); [Sov. Phys. Usp. **34**(7) 572 (1991)].
- [3] D.L. Aronstein and C.R. Stroud Jr., Phys. Rev. A **55** 4526 (1997).
- [4] Z. Dačić-Gaeta and C.R. Stroud, Jr., Phys. Rev. A **42** 6308 (1990);
J.C. Gay, D. Delande and A. Bommier, Phys. Rev. A **39** 6587 (1989);
M. Nauenberg, Phys. Rev. A **40**, 1133 (1989).
- [5] M. Nauenberg, C.R. Stroud, Jr. and J.A. Yeazell, Scientific American, June 1994, 24.
- [6] S.D. Boris, S. Brandt, H.D. Dahmen, T. Stroh, and M.L. Larsen, Phys. Rev. A **48** 2574 (1993).
- [7] R. Bluhm and V.A. Kostelecky, Phys. Rev. A **51** 4767 (1995).
- [8] R.M. Bowman, M. Dantus and A.H. Zewail, Chem. Phys. Lett. **161** 297 (1989).
- [9] M.J.J. Vrakking, D.M. Villeneuve and A. Stolow, Phys. Rev. A **54** R37 (1996).
- [10] R. Bluhm, V.A. Kostelecky and B. Tudose, Phys. Lett. A **222** 220 (1996).
- [11] R. Bluhm, V.A. Kostelecky and J.A. Porter, Am. J. Phys. **64** 944 (1996).
- [12] G. Alber and P. Zoller, Phys. Rep. **199** 231 (1991);
B.M. Garraway and K.A. Suominen, Rep. Prog. Phys. **58** 365 (1995).
- [13] J.R. Klauder and B.S. Skagerstam, *Coherent States*, (World Scientific, Singapore (1985)).
- [14] S.I. Vetchinkin, A.S. Vetchinkin, V.V. Eryomin and I.M. Umanskii, Chem. Phys. Lett. **215** 11 (1993).
- [15] J. Mostowski, Phys. Lett. A **56** 369 (1976).
- [16] P.W. Atkins and J.C. Dobson, Proc. Roy. Soc. Lond. A **321** 321 (1971).
- [17] J. Schwinger, in: *Quantum Theory of Angular Momentum*, L.C. Biedenharn and H. van Dam (eds.), Academic Press, New York (1965).
- [18] D. Janssen, Yad. Fiz. **25** 897 (1977), [Sov. J. Nucl. Phys. **25** 479 (1977)].
- [19] R. Arvieu and P. Rozmej, Phys. Rev. A **51** 104 (1995);
R. Arvieu, P. Rozmej and W. Berej, J. Phys. A **30** 5381 (1997).
- [20] R. Broglia and A. Winther, *Heavy Ion Reactions*, (Benjamin, New York (1981)).
- [21] L. Fonda, N. Mankoč-Borstnik and M. Rosina, Phys. Rep. **158** 159 (1988).
- [22] R. Bonifacio, D.M. Kim and M.O. Scully, Phys. Rev. **187** 441 (1969).
- [23] V.V. Mikhailov, Theor. Math. Phys. **15** 584 (1973); Phys. Lett. A **34** 343 (1971).
- [24] P. Gulshani, Can. J. Phys. **57** 998 (1979); **25** 479 (1977).
- [25] A.M. Perelomov, Commun. Math. Phys. **26** 222 (1972).
- [26] P.A. Braun and V.I. Savichev, Phys. Rev. A **49** 1704 (1994).
- [27] F. Grossmann, J.M. Rost and W.P. Schleich, J. Phys. A **30** L277 (1997).
- [28] M. Persico and P. Van Leuven, Z. Phys. D **41** 139 (1997).
- [29] R. Arvieu and P. Rozmej, (to be published).

Figure captions

FIG. 1. Probabilities to find the partial waves Y_l^J in the coherent states of Mostowski (solid line) and Atkins–Dobson (dashed impulses) for parameters $N = 20 = 1/2(k^2 + 1)$ ensuring the same angular velocity for both wave packets.

FIG. 2. Time evolution of Mostowski’s wave packet for diatomic molecule with $N = 20$. The left column represents changes of the probability density during short term evolution, the right one at fractional revival times. The probability density at times equal $1/5, 1/3$ and $1/2 * T_{rev}$ are identical with those presented at $1/10, 1/6$ and $n * T_{rev}$, respectively. (The vertical scale is not the same in all figures.)

FIG. 3. Time evolution of Mostowski’s wave packet with $N = 20$. The $|\Psi_M(\theta, \phi, t)|^2$ for fixed $\theta = \pi/2$ is presented in the contour plot. The larger values of $|\Psi_M(\theta, \phi, t)|^2$ result in heavy lines due to almost overlapping cuts for fractional revivals. One can clearly see the fractional revivals of orders $1/7, 1/12, 1/5, 1/8, 1/6, 1/4$ and so on (corresponding times are $1/7, 1/6, 1/5, 1/4, 1/3$ and $1/2$ of T_{rev}).

FIG. 4. Time evolution of the wave packet (34) for $N = 50$ for diatomic molecule. The probability density $2\pi \sin \theta |\Psi|^2$ is presented in the contour plot. The larger values of $2\pi \sin \theta |\Psi|^2$ result in heavy lines due to almost overlapping cuts for fractional revivals.

FIG. 5. Time evolution of the Ψ_{cl} (39) for $N = 50$. The probability density $2\pi \sin \theta |\Psi_{cl}|^2$ is presented as a function of θ and t within one classical period.

FIG. 6. The autocorrelation function for $N = 20$ and different values of parameter η corresponding to a smooth transition between two different symmetries.

FIG. 7. Transition of fractional wave packets from exact clones ($\eta = 1$) through developing crescents ($\eta = 1/2, \eta = 1/4$) to ring topology ($\eta = 0$) is demonstrated for two fractional revival times $t = 1/3 * T_{rev}$ (left) and $t = 1/4 * T_{rev}$ (right). The fractional waves called mutants are clearly seen in the lower rows of the figure.

FIG. 8. Time evolution of the coherent state deduced from elliptic motion ($\eta = 0.5$). The time sequence presented here is the same as in Fig. 2. Comparing to this figure the crescents are clearly visible, they are the most pronounced for $t = \frac{1}{4} T_{rev}$.

FIG. 9. Time evolution of Janssen’s coherent state for axially symmetric top (75) for irrational $\delta = 1/\sqrt{3}$ implying $T_{rev}^I = 1/\sqrt{3} T_{rev}^K \simeq 0.577 T_{rev}^K$. Shown is the probability density $|\langle \alpha \beta \gamma | \bar{I} \bar{K} \rangle|^2$ for $\beta = \pi/2, \bar{I} = 4$ and $\bar{K} = 0$. Notice that the vertical scale is not the same in all figures.

FIG. 10. The same as in Fig. 9 but for rational $\delta = 1/2$ implying $T_{rev}^{I,K} = T_{rev}^K = 2 T_{rev}^I$. Clones for times $1/6, 1/3$ and $1/2 T_{rev}^{I,K}$ are clearly visible as well as full revivals. Notice that the vertical scale is not the same in all figures.

Figures

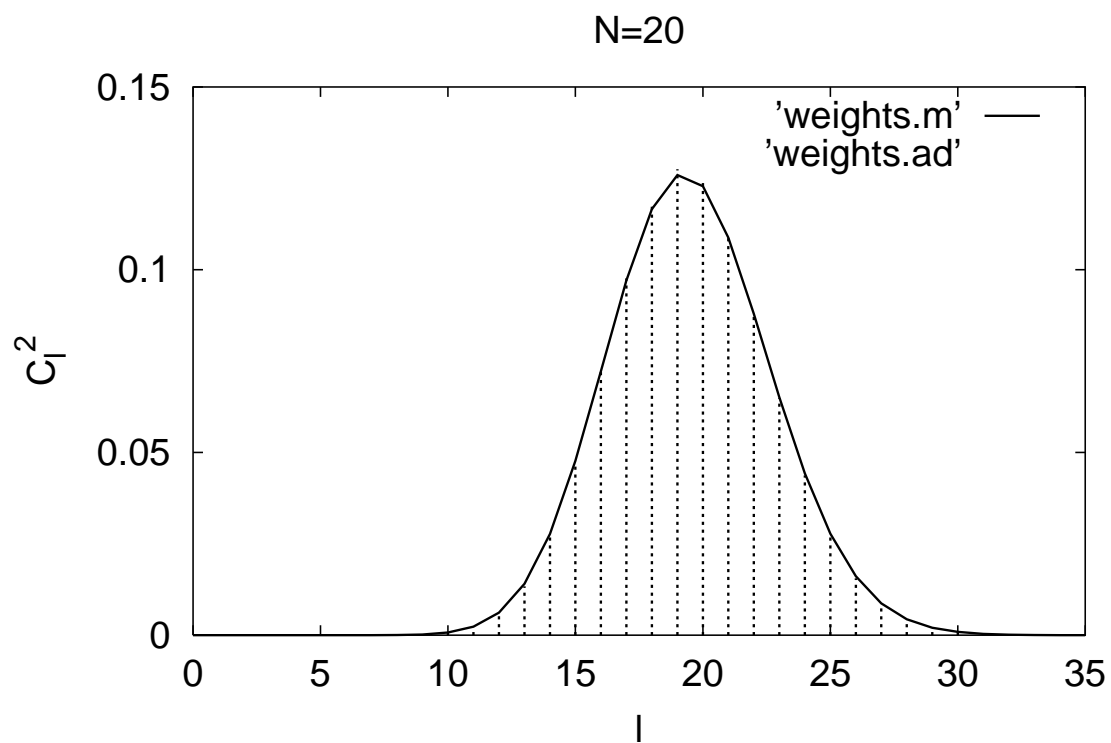


Figure 1: Probabilities to find the partial waves Y_l^I in the coherent states of Mostowski (solid line) and Atkins–Dobson (dashed impulses) for parameters $N = 20 = 1/2(k^2 + 1)$ ensuring the same angular velocity for both wave packets.

$N=20 \quad \eta=1$

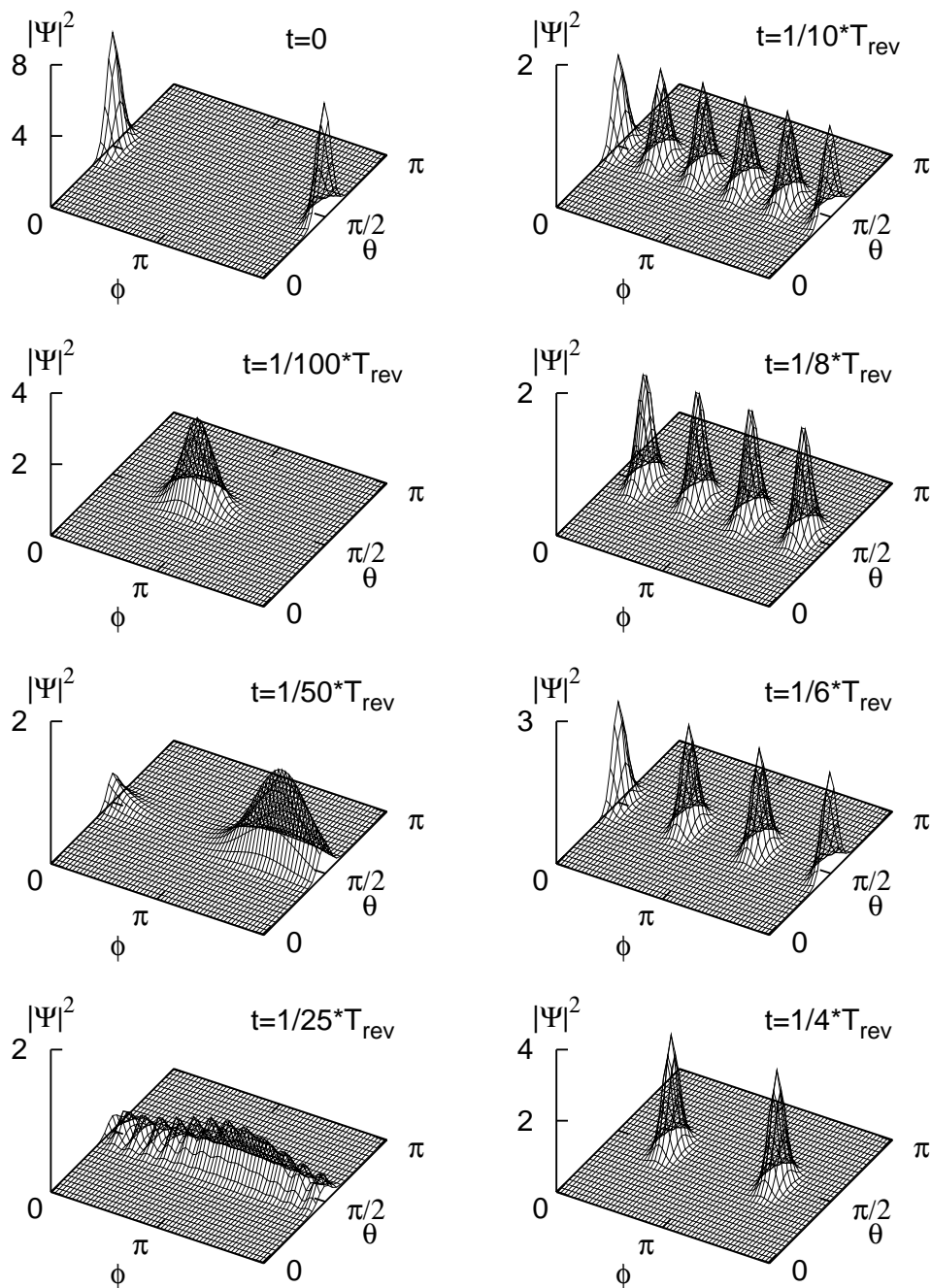


Figure 2: Time evolution of Mostowski's wave packet for diatomic molecule with $N = 20$. The left column represents changes of the probability density during short term evolution, the right one at fractional revival times. The probability density at times equal $1/5$, $1/3$ and $1/2 * T_{rev}$ are identical with those presented at $1/10$, $1/6$ and $n * T_{rev}$, respectively. (The vertical scale is not the same in all figures.)

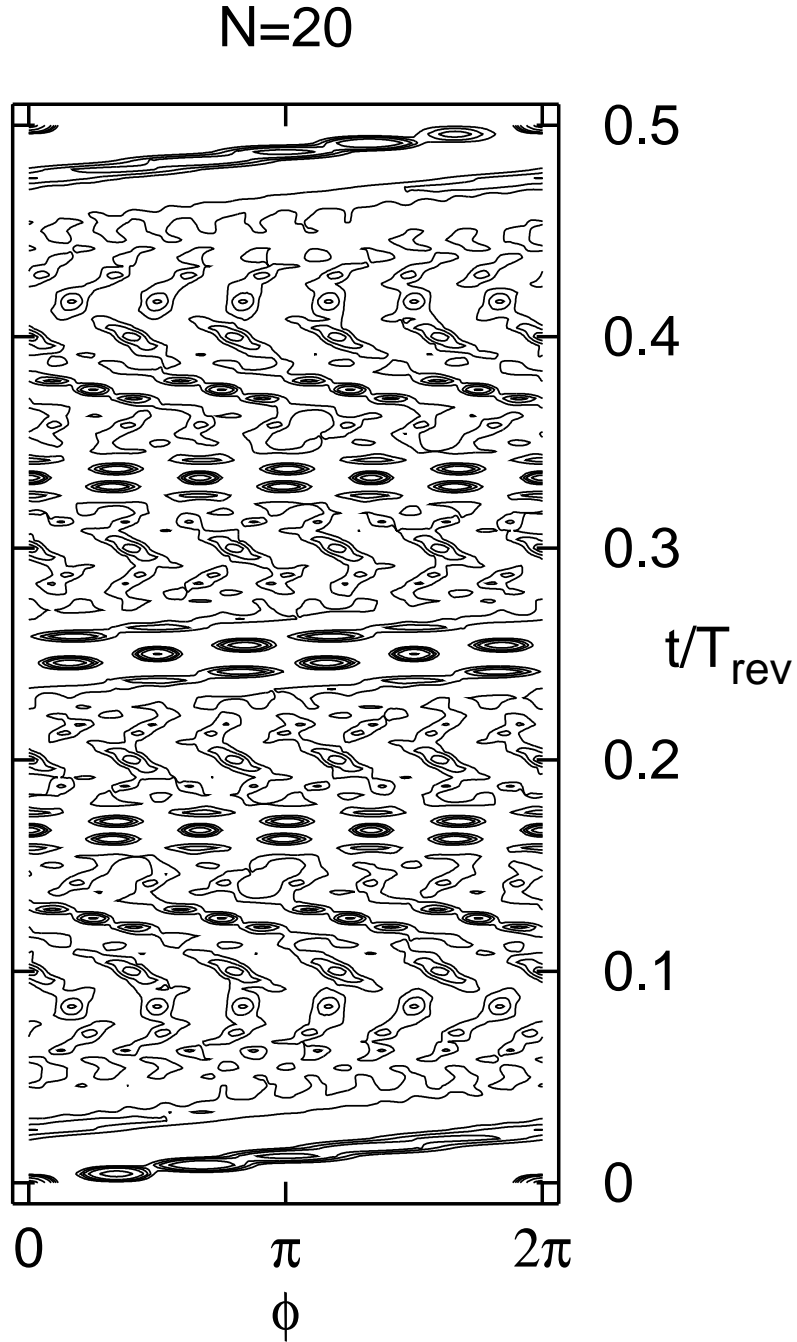


Figure 3: Time evolution of Mostowski's wave packet with $N = 20$. The $|\Psi_M(\theta, \phi, t)|^2$ for fixed $\theta = \pi/2$ is presented in the contour plot. The larger values of $|\Psi_M(\theta, \phi, t)|^2$ result in heavy lines due to almost overlapping cuts for fractional revivals. One can clearly see the fractional revivals of orders $1/7, 1/12, 1/5, 1/8, 1/6, 1/4$ and so on (corresponding times are $1/7, 1/6, 1/5, 1/4, 1/3$ and $1/2$ of T_{rev}).

Linear WP, N=50

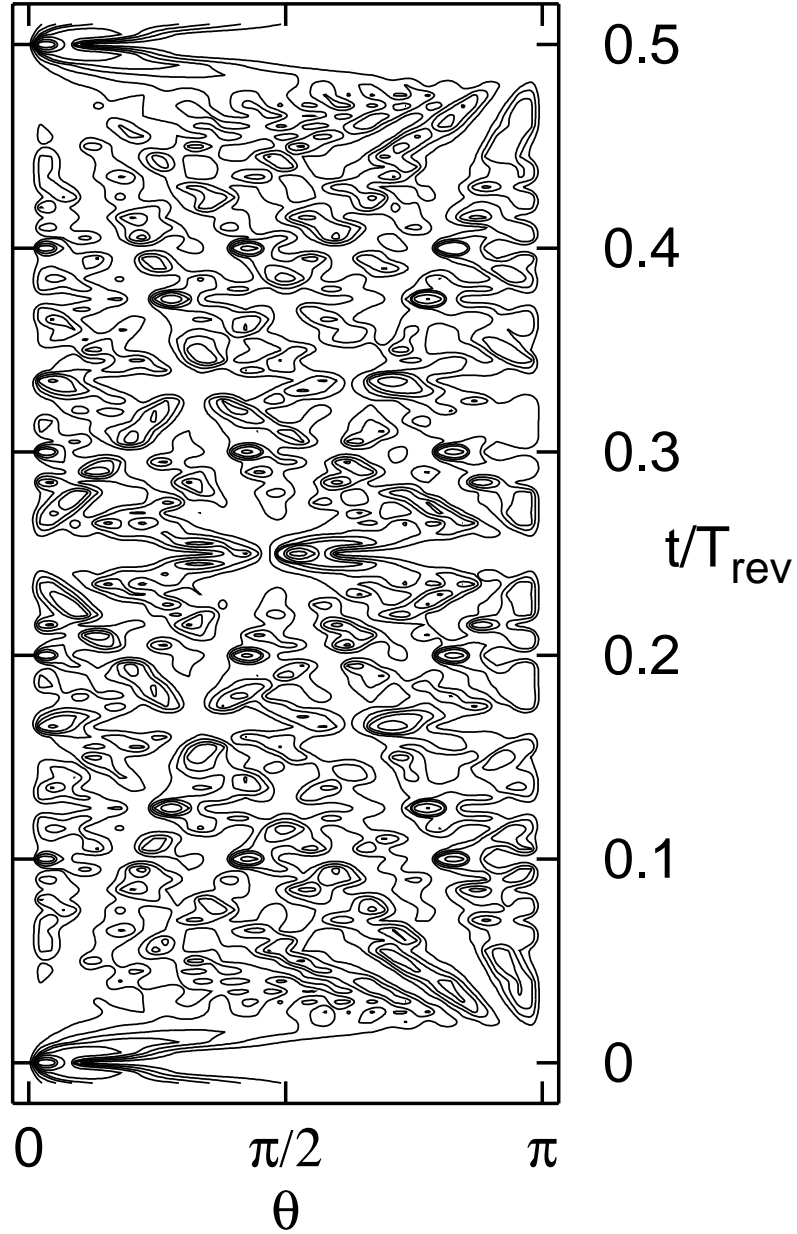


Figure 4: Time evolution of the wave packet (34) for $N = 50$ for diatomic molecule. The probability density $2\pi \sin \theta |\Psi|^2$ is presented in the contour plot. The larger values of $2\pi \sin \theta |\Psi|^2$ result in heavy lines due to almost overlapping cuts for fractional revivals.

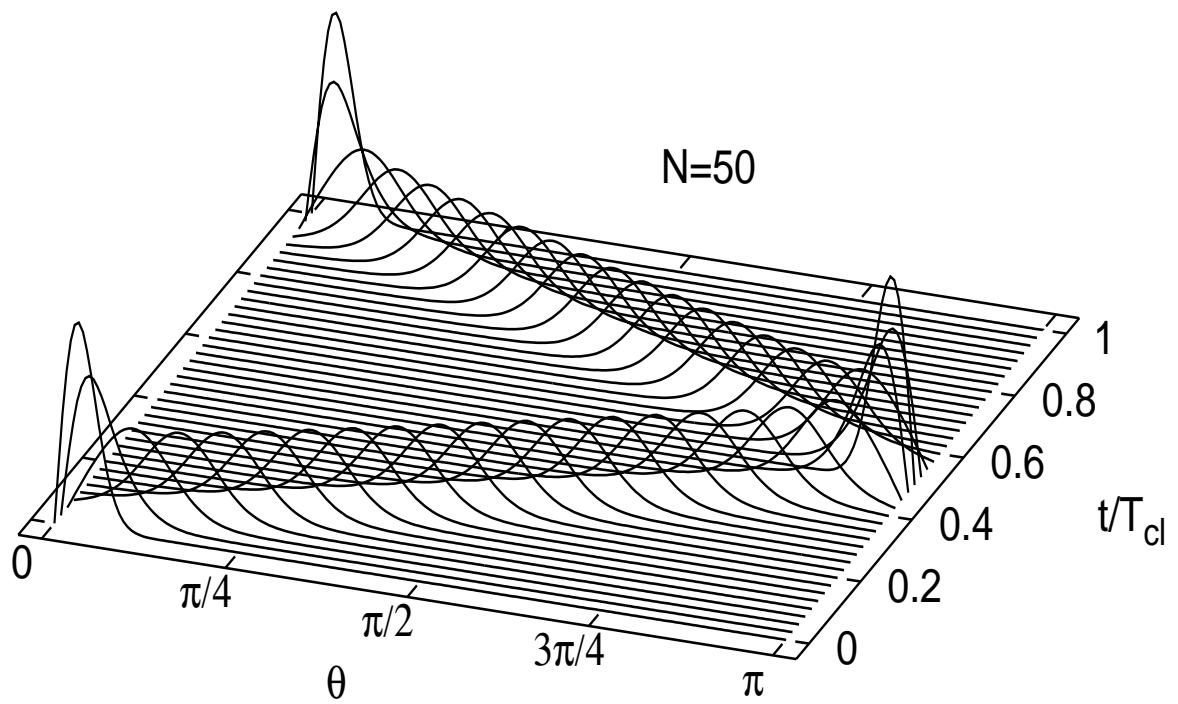


Figure 5: Time evolution of the Ψ_{cl} (39) for $N = 50$. The probability density $2\pi \sin \theta |\Psi_{cl}|^2$ is presented as a function of θ and t within one classical period.

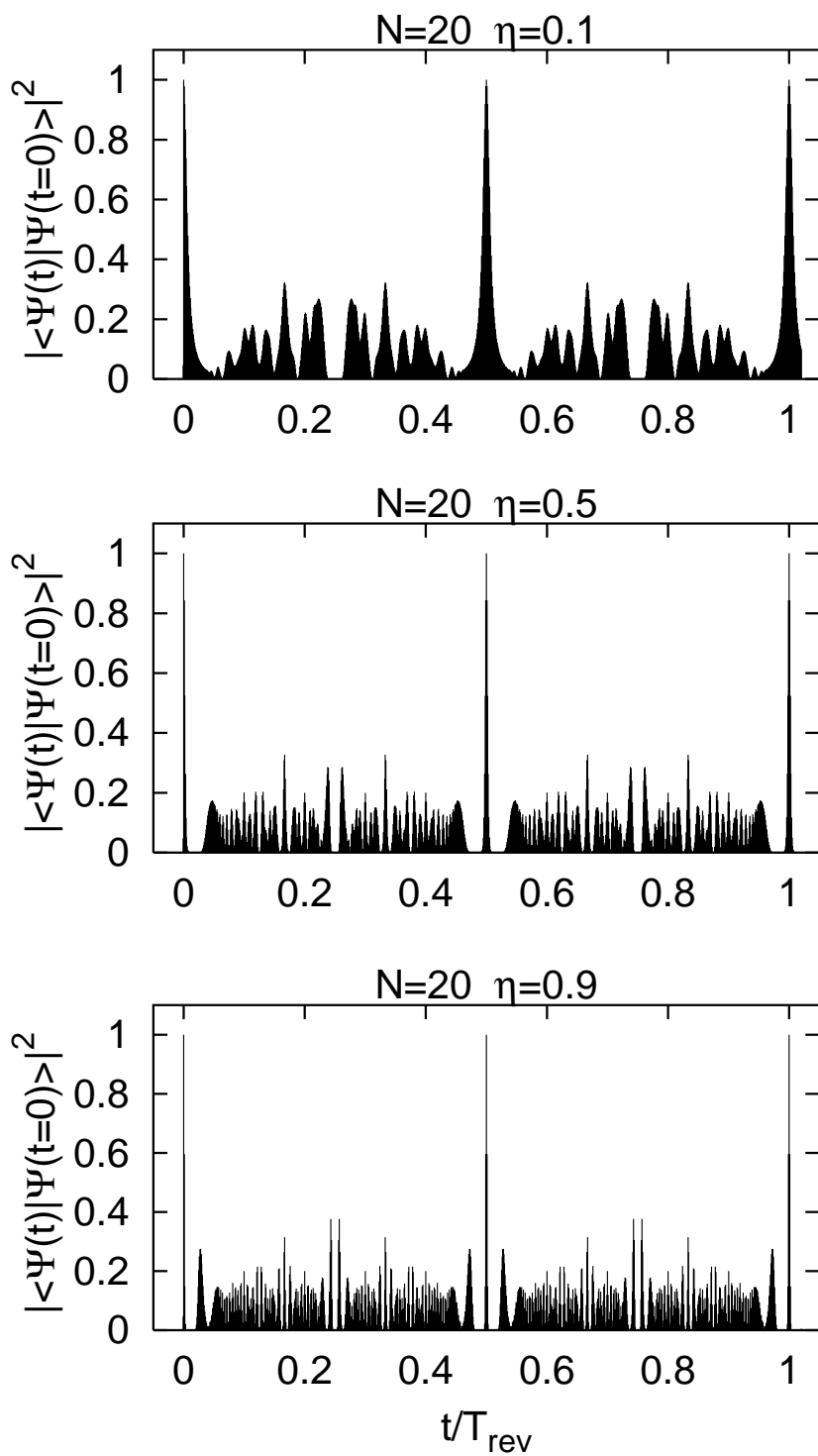


Figure 6: The autocorrelation function for $N = 20$ and different values of parameter η corresponding to a smooth transition between two different symmetries.

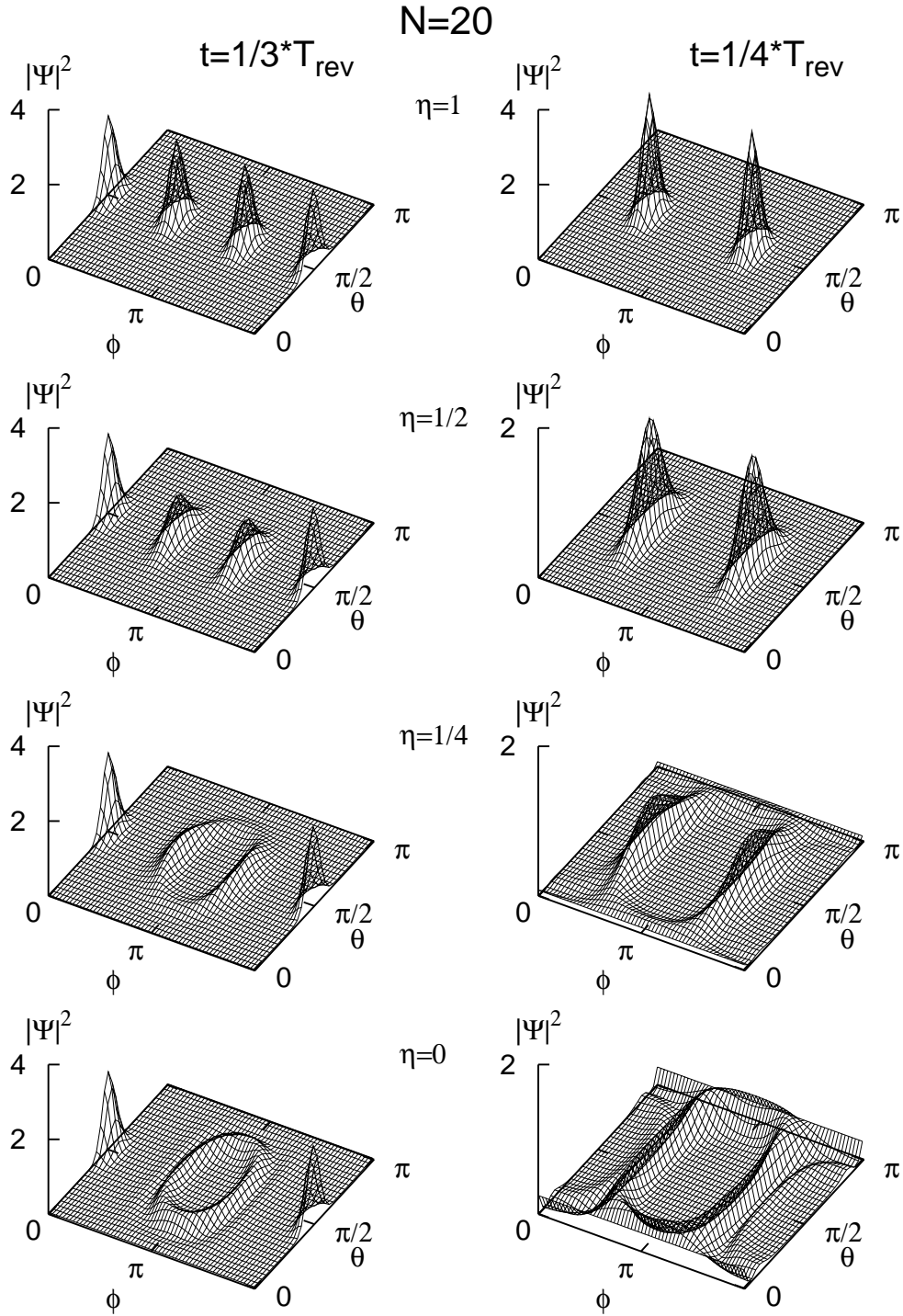


Figure 7: Transition of fractional wave packets from exact clones ($\eta = 1$) through developing crescents ($\eta = 1/2, \eta = 1/4$) to ring topology ($\eta = 0$) is demonstrated for two fractional revival times $t = 1/3 * T_{rev}$ (left) and $t = 1/4 * T_{rev}$ (right). The fractional waves called mutants are clearly seen in the lower rows of the figure.

$N=20 \quad \eta=0.5$

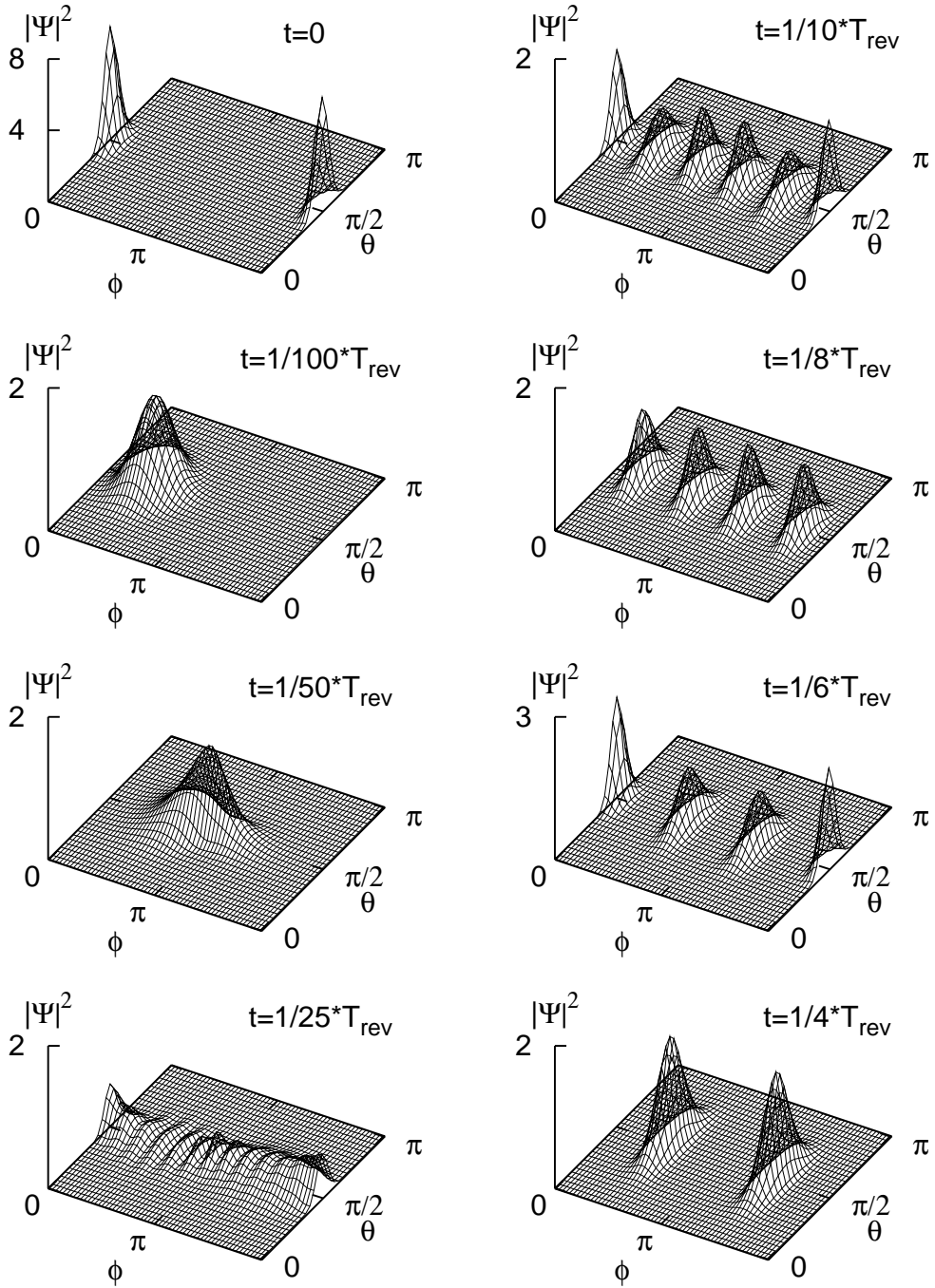


Figure 8: Time evolution of the coherent state deduced from elliptic motion ($\eta = 0.5$). The time sequence presented here is the same as in Fig. 2. Comparing to this figure the crescents are clearly visible, they are the most pronounced for $t = \frac{1}{4} T_{rev}$.

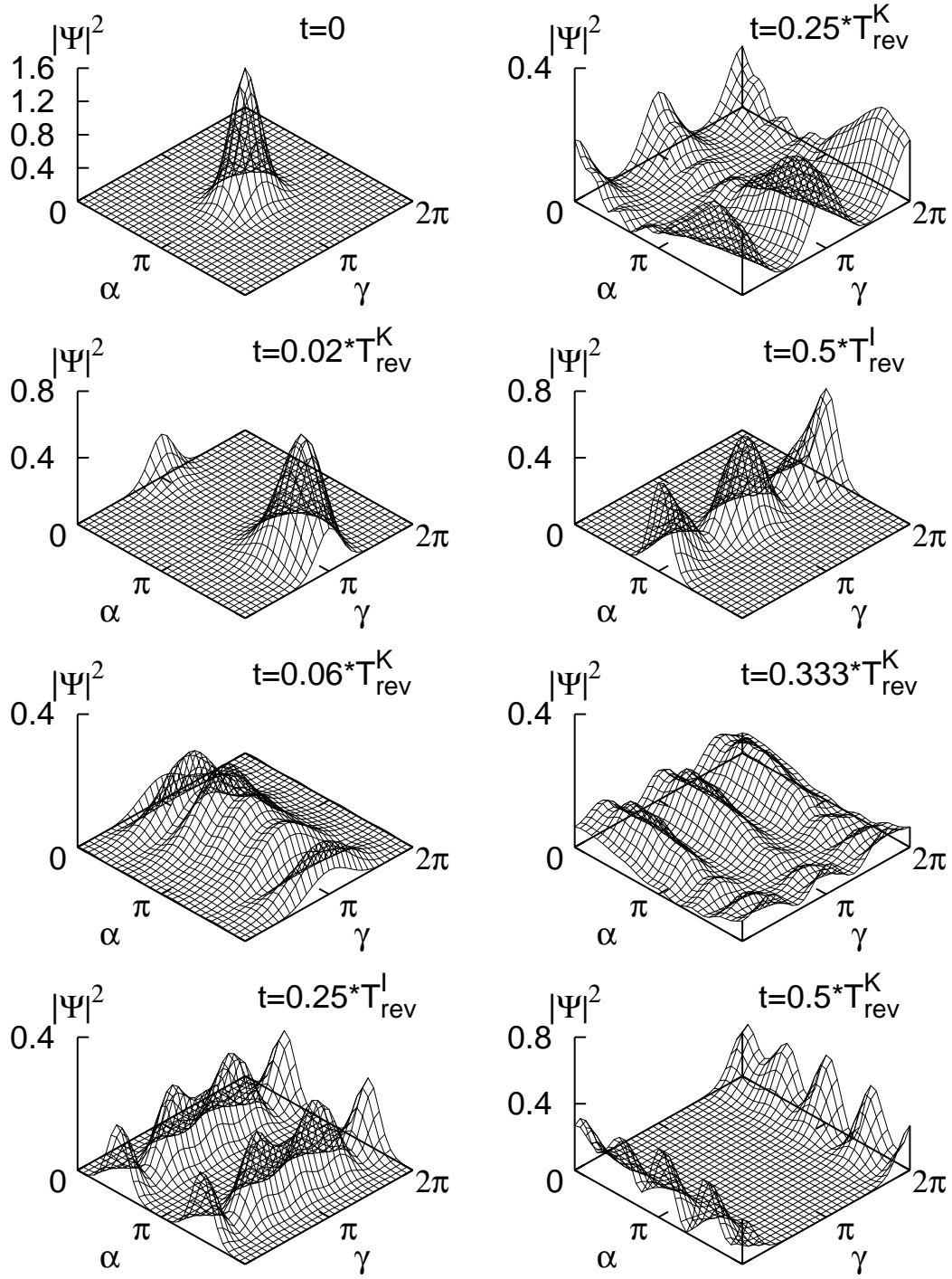


Figure 9: Time evolution of Janssen's coherent state for axially symmetric to (75) for irrational $\delta = 1/\sqrt{3}$ implying $T_{rev}^I = 1/\sqrt{3} T_{rev}^K \simeq 0.577 T_{rev}^K$. Shown is the probability density $|\langle \alpha\beta\gamma | \bar{I}\bar{K} \rangle|^2$ for $\beta = \pi/2$, $\bar{I} = 4$ and $\bar{K} = 0$. Notice that the vertical scale is not the same in all figures.

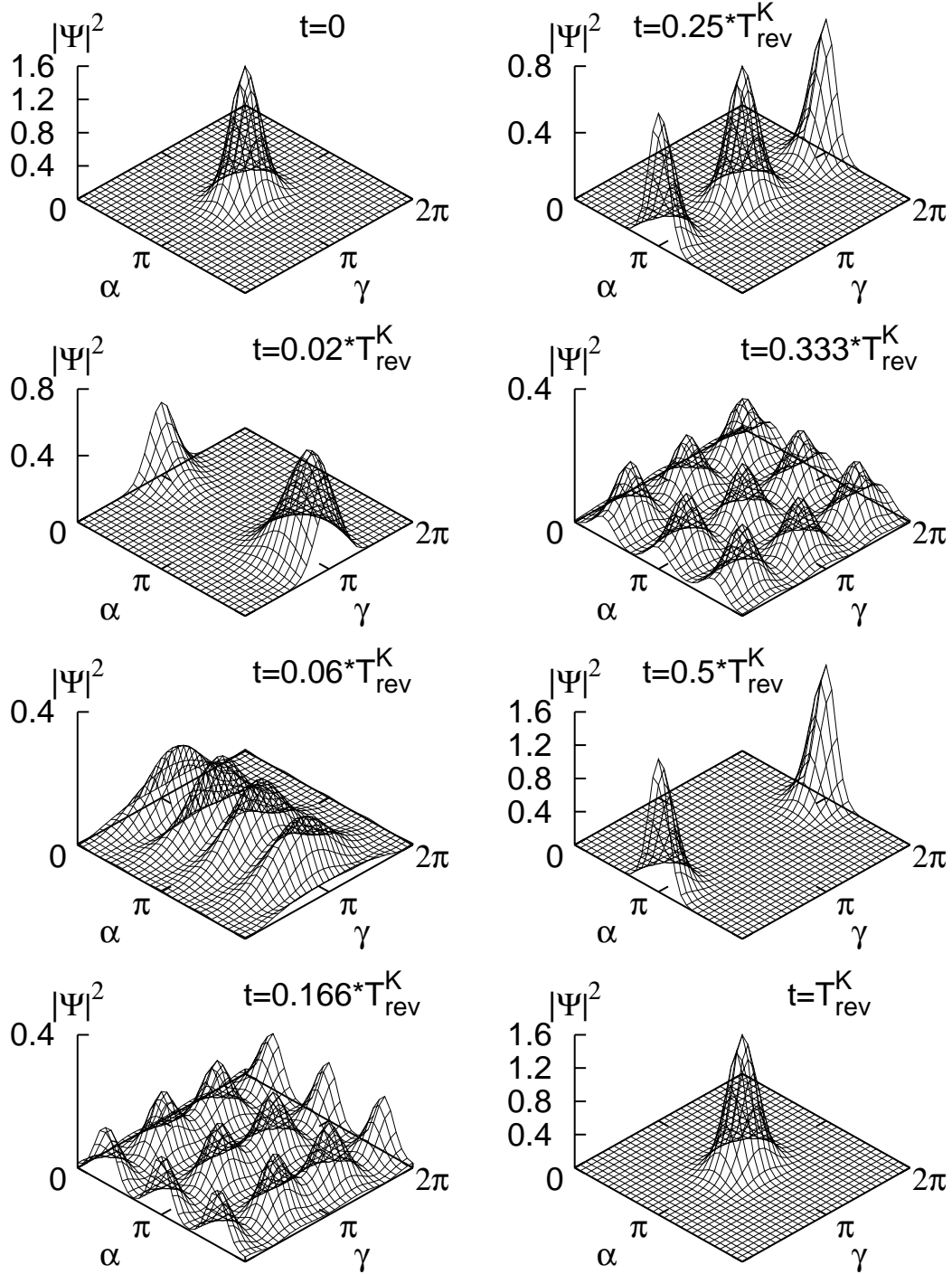


Figure 10: The same as in Fig. 9 but for rational $\delta = 1/2$ implying $T_{rev}^{I,K} = T_{rev}^K = 2T_{rev}^I$. Clones for times $1/6$, $1/3$ and $1/2 T_{rev}^{I,K}$ are clearly visible as well as full revivals. Notice that the vertical scale is not the same in all figures.